Taiebat, H. A. and Carter, J. P. (2000). *Géotechnique* **50**, No. 4, 409–418

Numerical studies of the bearing capacity of shallow foundations on cohesive soil subjected to combined loading

H. A. TAIEBAT* and J. P. CARTER*

This paper presents the results of three-dimensional finite-element analyses of circular foundations on the surface of homogeneous, purely cohesive soil. The foundations were assumed to adhere fully to the soil, and compressive, tensile and shear stresses may develop at the interface between the footing and the soil. The predicted ultimate response of the foundations to combined vertical, moment and horizontal loading was compared with other available theoretical predictions. A three-dimensional failure locus is presented for these foundations, based on the numerical predictions. An equation that approximates the shape of the failure locus is also suggested, and this provides a convenient means of calculating the bearing capacity of circular foundations on a uniform clay and subjected to combined loading.

KEYWORDS: bearing capacity; footings/foundations; numerical modelling and analysis.

Cet exposé présente les résultats d'analyses d'éléments finis en trois dimensions pour des fondations circulaires sur la surface d'un sol homogène purement cohésif. Nous avons présumé que les fondations adhéraient totalement au sol et que des contraintes de compression, de traction et de cisaillement pourraient se développer à l'interface entre le sol et le pied des fondations. Nous avons comparé leur réaction ultime prévue face à la charge de verticale, de moment et d'horizontale avec d'autres prévisions théoriques. Nous présentons un point de défaillance en trois dimensions pour ces fondations en nous basant sur les prévisions numériques. Nous suggérons aussi une équation approximative pour la forme du point de défaillance, équation qui constitue un moyen pratique de calculer la capacité porteuse de fondations circulaires sur une argile uniforme, soumises à des charges combinées.

INTRODUCTION

The bearing capacity of foundations has always been one of the subjects of major interest in soil mechanics and foundation engineering. There is an extensive literature dealing with the bearing capacity of foundations, from both theoretical and experimental standpoints. A list of principal contributions to this subject can be found in Vesic (1973), Chen & McCarron (1991) and Tani & Craig (1995). Most of the design methods for estimating bearing capacity are based on the original studies of a strip punch done by Prandtl (1921) and Reissner (1924), modified to accommodate the conditions not included in the Prandtl–Reissner solution, such as load inclination, footing shape, etc. The modifications are usually based on either limit equilibirum analyses or empirical approaches. These conventional design methods provide simple and effective tools for estimating the bearing capacity of foundations under predominantly vertical loading. However, for foundations under substantial moment and lateral load, these methods may not provide theoretically rigorous or practically reliable solutions.

In addition to the conventional methods, attempts have been made in the last decade to define failure loci and interaction equations for foundations using more rigorous methods. A failure locus defines the load conditions under which failure of a foundation occurs. Any combination of loads inside the failure locus is regarded to be safe for the foundation. These newer methods have been supported by a large number of experiments on model-scale shallow footings, carried out by many researchers, among them Osborne *et al*. (1991), Butterfield & Gottardi (1994) and Martin (1994). Some of the proposed failure equations are based on theoretical and numerical analysis (e.g. Murff, 1994; Bransby & Randolph, 1998).

In this paper, the results of a series of three-dimensional finite-element analyses of a circular foundation resting on the surface of a cohesive soil are used to find a failure envelope for the foundation. The results of the numerical analyses are compared with the conventional bearing-capacity equation and some of the other failure loci proposed for cohesive soil. An important feature of the problem considered is that unlimited tensile stress is permitted at the interface between the soil and the foundation under large-moment loading.

Manuscript received 28 June 1999; revised manuscript accepted 20 February 2000.
Discussion on this paper closes 26 November 2000; for further details see p. ii.
*The University of Sydney.

FAILURE EQUATIONS

Some of the failure equations proposed for foundations on cohesive soil are discussed here. At least two classes of the failure equations can be identified. In the first, the conventional bearing-capacity equations, it is assumed that the footing–soil interface cannot sustain any tension. In the second class of failure equations some resistance to tension is allowed, and therefore these equations are more relevant to the present studies.

The conventional bearing-capacity equations (e.g. Vesic, 1975; Bowles, 1982; Chen & McCarron, 1991) are generally used to evaluate the stability of foundations against static bearing failure. The bearing capacity of a rigid surface foundation resting on a purely cohesive soil and subjected to a vertical loading may be expressed approximately as (Vesic, 1975)

$$V_u = s_u N_c \zeta_s \zeta_e \zeta_i A \tag{1}$$

where V_u is the ultimate vertical load on the foundation, s_u is the undrained shear strength of the soil, N_c is the dimensionless bearing capacity factor for cohesion, ζ_s is the factor which considers the effects of foundation shape, ζ_e and ζ_i are factors which consider the effects of load eccentricity and load inclination, and A is the contact area of the foundation.

The bearing capacity factor N_c for a long rectangular foundation has been obtained as $N_c = 2 + \pi$ using the theory of plasticity. The values of shape factor ζ_s for a circular footing vary from 1·1 (e.g. Meyerhof, 1980) to 1·3 (e.g. Terzaghi & Peck, 1948). A widely used expression for the shape factor (Vesic, 1975) suggests a value of 1·2 for circular footings. Therefore, the ultimate bearing capacity of circular foundations on clay under a central–vertical load V_u is conventionally calculated as

$$V_u = 1{\cdot}2(2 + \pi) A s_u \approx 6{\cdot}17\, A s_u \tag{2}$$

It is worth noting that exact solutions for the vertical bearing capacity of circular footings on uniform Tresca soil have been obtained by many researchers (e.g. Meyerhof, 1951; Shield, 1955; Eason & Shield, 1960; Cox, 1961; Cox *et al*., 1961). Values of $V_u = 5{\cdot}69 A s_u$ and $V_u = 6{\cdot}05 A s_u$ have usually been

obtained for smooth and fully rough circular footings, respectively. Therefore, the appropriate shape factors are 1·11 and 1·18 for smooth and rough circular footings. It should also be pointed out that very different shape factors have been obtained for non-uniform soil (e.g. Tani & Craig, 1995).

There is no exact expression for evaluating the effects of inclination and eccentricity of the load applied to a circular foundation. However, Vesic (1975) has presented an approximate expression for the bearing capacity of rectangular foundations, with an aspect ratio B/L, subjected to inclined loading. Using Vesic's expression and assuming $B/L = 1$, an approximate bearing-capacity equation for circular footings under inclined loading can be obtained as follows:

$$\frac{V}{A} = 1{\cdot}2\left[(2+\pi)s_u - 1{\cdot}5\frac{H}{A}\right] \tag{3}$$

where H is the horizontal component of the applied load.

Bolton (1979) presented a theoretical expression for the vertical capacity of a strip footing subjected to an inclined load. Bolton's expression can be modified for a circular footing, using a shape factor $\zeta_s = 1{\cdot}2$, as follows:

$$\frac{V}{A} = 1{\cdot}2\ s_u\left[1+\pi - \arcsin\left(\frac{H}{As_u}\right) + \sqrt{1-\left(\frac{H}{As_u}\right)^2}\right] \tag{4}$$

Based on the results of empirical studies on circular foundations performed by Osborne *et al*., (1991), Murff (1994) suggested a general form of the three-dimensional failure locus as:

$$\sqrt{\left(\frac{M}{D}\right)^2 + \alpha_1 H^2} + \alpha_2\left[\frac{V^2}{V_c} - V\left(1+\frac{V_t}{V_c}\right) + V_t\right] = 0 \tag{5}$$

where α_1 and α_2 are constants, M is the moment applied to the foundation, V_c is the compression capacity under pure vertical load, and V_t is the tension capacity of the footing, which might be possible to mobilize in practice, at least in the short-term, due to the development of suction under the footing. A simple form of equation (5), suitable for foundations on saturated cohesive soil under fast loading (undrained conditions), assuming $V_t = -V_c = -V_u$, is

$$\sqrt{\left(\frac{M}{\alpha_3 V_u D}\right)^2 + \left(\frac{H}{\alpha_4 V_u}\right)^2} + \left(\frac{V}{V_u}\right)^2 - 1 = 0 \tag{6}$$

$\alpha_3 V_u D$ and $\alpha_4 V_u$ can be seen as the capacity of the foundation under pure moment M_u and pure horizontal load H_u, respectively. Therefore equation (6) can also be expressed as

$$\sqrt{\left(\frac{M}{M_u}\right)^2 + \left(\frac{H}{H_u}\right)^2} + \left(\frac{V}{V_u}\right)^2 - 1 = 0 \tag{7}$$

A finite-element study of the failure locus for strip foundations on non-homogeneous clay under combined loading was presented by Bransby & Randolph (1998). The results of the finite-element analyses were supported by upper-bound plasticity analyses. The failure locus presented by Bransby & Randolph is

$$\left(\frac{V}{V_u}\right)^2 + \sqrt[\alpha_3]{\left(\frac{M^*}{M_u}\right)^{\alpha_1} + \left(\frac{H}{H_u}\right)^{\alpha_2}} - 1 = 0 \tag{8}$$

in which

$$\frac{M^*}{ABs_{u0}} = \frac{M}{ABs_{u0}} - \frac{Z}{B}\frac{H}{As_{u0}} \tag{9}$$

where M^* is the moment calculated about a reference point above the base of the footing at a height Z, B is the breadth of the strip footing, α_1, α_2 and α_3 are factors depending on the degree of non-homogeneity of the soil, and s_{u0} is the soil shear strength at the level of the foundation base.

FINITE-ELEMENT MODEL

Three-dimensional finite-element analysis of a circular foundation resting on the surface of homogeneous soil deforming under undrained conditions were performed to investigate the shape of the failure envelope in the vertical–horizontal–moment (VHM) space for the circular foundation. It was assumed that the soil–foundation interface provides uplift resistance, which in practice may be due to the suctions that can be developed during undrained loading. The emphasis of the study was on assessing the effects of lateral force and moment on the vertical bearing capacity of the foundation.

The soil was assumed to have a uniform undrained shear strength s_u and an undrained Young's modulus E_u of 300 s_u. A Poisson's ratio of 0·5 (in practice $\nu = 0{\cdot}49$ to avoid numerical difficulties) was assumed to model the constant-volume elastic response of the soil under undrained conditions. During plastic yielding the soil also deforms at constant volume.

The finite-element mesh used in the analyses is shown in Fig. 1, which also defines the overall geometry of the finite-element model. The footing was assumed to be rigid and rough. A thin layer of continuum elements was used in the region of the soil–foundation interface, which considerably improved the predictions of the lateral response of the foundation. No attempt was made to model the separation of the footing from the soil, which may occur on the tension side of the footing under large moments.

The finite-element formulation used in the analyses is based on the semi-analytical approach (Zienkiewicz & Taylor, 1989) in which the field quantities are approximated by a discrete Fourier representation (Taiebat, 1999). This approach is similar to one described previously by Lai & Booker (1991). The material non-linearity is also represented by the elastic–perfectly-plastic Tresca failure criterion. Application of this method to problems with axisymmetric geometry which are subjected to non-symmetric loading has shown an effective reduction in computational time. For the mesh presented in Fig. 1, the computational time is about 5% of the time required for an equivalent three-dimensional finite-element analysis with the direct representation of the field quantities.

The sign conventions for loads and moment used in this study were based on the right-handed axes and clockwise positive conventions (V, M, H), as described by Butterfield *et al*. (1997) and shown in Fig. 2.

FAILURE POINT

In all the finite-element analyses reported here the loading was specified by increasing the total nodal force applied to the rigid footing (i.e. it was load-defined rather than displacement defined). This poses special problems for the determination of the ultimate capacity, as explained below.

In load-defined elastoplastic finite-element analyses of foun-

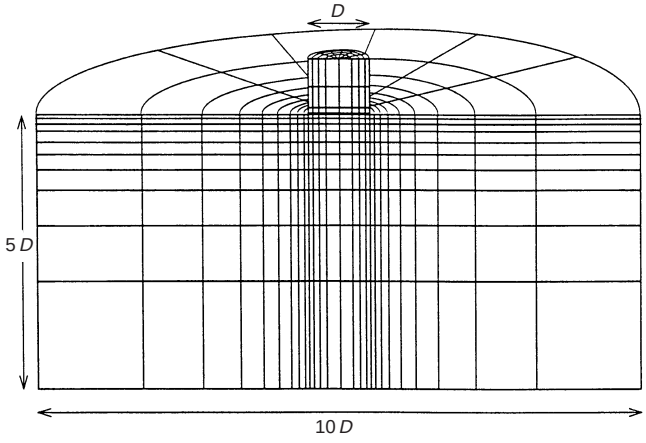

Fig. 1. Finite-element mesh and the geometry of the problem

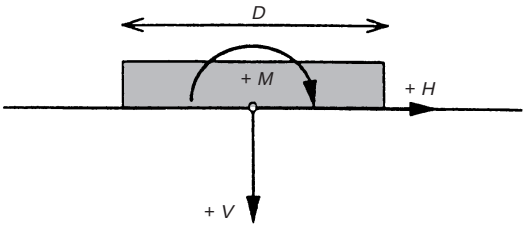

Fig. 2. Conventions for loads and moment on circular foundations

dations subjected to vertical load, it is very difficult to find a point at which overall failure can be deemed to occur. This difficulty arises because there may not be a point at which the numerical prediction of the incremental system stiffness is precisely zero, due to gradual development of the plastic zone. However, under horizontal load, failure is usually more sudden and therefore quite distinct. It coincides with the failure of the last Gauss point of the soil elements on or near the soil–foundation interface. Therefore, with any combination of horizontal load, vertical load and moment, an indication of the failure point can be best determined from the horizontal load–displacement curve. The failure of foundations under pure vertical load and pure moment is also best determined approximately by using a combination of a very low value of horizontal load and an applied vertical load or moment. As an example, the load–displacement response of a foundation under vertical and horizontal loading is presented non-dimensionally in Fig. 3, where δ represents the horizontal and vertical displacement. The horizontal or vertical loads were caluclated based on the stresses predicted in elements at the interface of the soil and the foundation. For any load combination the horizontal load–displacement curve exhibits a peak and thereafter the horizontal load decreases. The loads corresponding to the peak are regarded as 'failure loads'. In the present case the 'failure loads' were determined at $H = 0{\cdot}114\ As_u$ and $V = 5{\cdot}7\ As_u$.

TWO-DIMENSIONAL FAILURE ENVELOPES

Vertical–horizontal (VH) loading plane

The ultimate vertical load capacity of the foundation V_u was obtained from the results of finite-elements analysis with $V/H = 60$ and $M = 0$. The small horizontal component of the load was used to define better the ultimate load point, as described in the previous section. A value of $V_u = 5{\cdot}7\ As_u$ was deduced for the ultimate vertical bearing capacity of the circular foundation. This value is very close to the exact solution of $V_u = 5{\cdot}69\ As_u$ for a smooth circular footing on the surface of a rigid plastic half-space.

To evaluate any possible effect of the horizontal load of $H = V/60$ on the vertical bearing capacity, another analysis with a lower value of horizontal load, $H = V/600$, was carried out. The same value for the ultimate vertical bearing capacity was obtained, indicating the negligible influence of these relatively small horizontal loads on the vertical capacity of the footing.

The capacity of the foundation under pure horizontal load was predicted by the finite-element model to be $H_u = 1{\cdot}02\ As_u$, which compares well with the exact solution of $H_u = 1{\cdot}0\ As_u$.

The predicted failure envelope in the *VH* plane is presented in Fig. 4, together with the conventional solution of Vesic (1975) (equation (3)) and the modified expression of Bolton (1979) (equation (4)). Comparison of the curves in Fig 4 shows that the numerical analyses generally give a more conservative bearing capacity for foundations subjected to inclined load. The results of the numerical analyses are very close to the results obtained with the modified theoretical expression of Bolton (1979).

All three methods indicate that there is a critical angle of inclination, measured from the vertical direction, above which the ultimate horizontal resistance of the foundation dictates the failure of the foundation. Where the inclination angle is more than the critical value, the vertical force does not have any influence on the horizontal capacity of the foundation. The critical angle is predicted to be 19° by the numerical studies and from the modified expression of Bolton (1979), compared to 13° predicted by the conventional method of Vesic (1975).

The non-dimensional failure envelope predicted in the present numerical analyses is compared with those of Vesic (1975) (equation (3)), Bolton (1979) (equation (4)), Murff (1994) (equation (7)) and Bransby & Randolph (1998) (equation (8)) in Fig. 5. The shape of the failure locus predicted by the numerical analyses is closest to the modified expression of Bolton (1979). It can be seen that the conventional method, compared with the numerical results, gives a good approximation of the failure locus, except at high values of horizontal loads. The failure locus presented by Murff (1994) gives a very conservative approximation of the numerical and conventional failure loci.

Vertical-moment (VM) loading plane

For the foundation under pure moment, an ultimate capacity of $M_u = 0{\cdot}8ADs_u$ is obtained from the results of the finite-

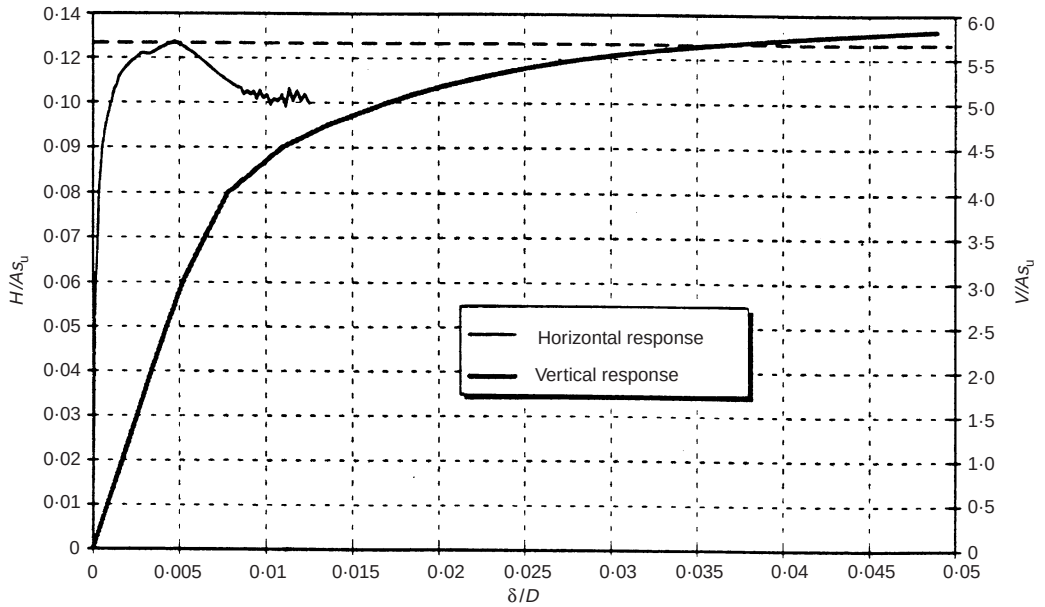

Fig. 3. Load–displacement response of the foundation under vertical and horizontal loading

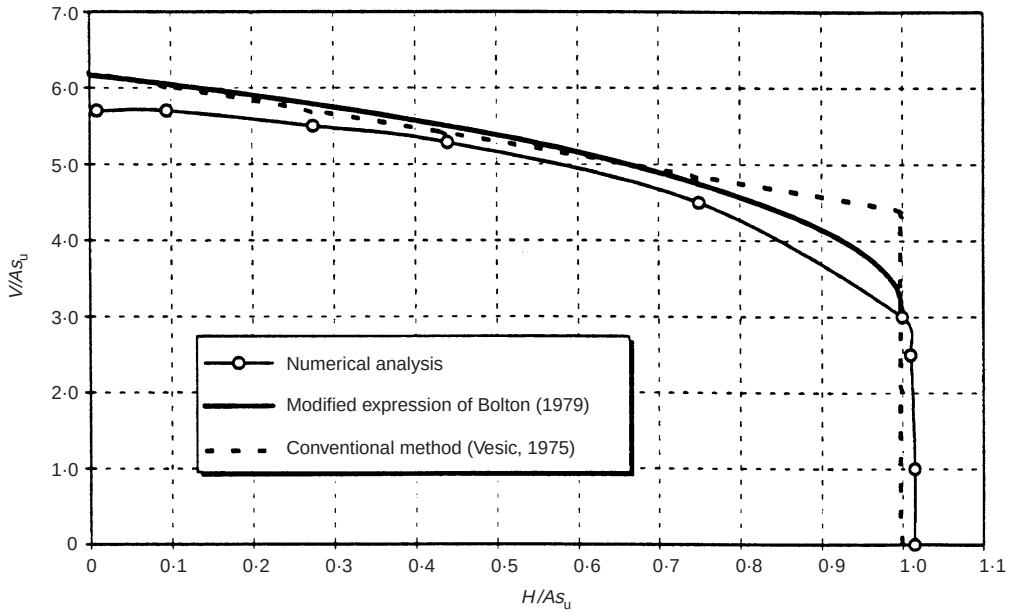

Fig. 4. Failure loci for foundations under inclined loading ($M = 0$)

element analysis, after assuming $M/H = 100$ and $V = 0$. No independent data are available to check the validity of this result.

The non-dimensional failure envelope predicted in the present numerical studies is compared with those of Murff (1994) (equation (7)) and Bransby & Randolph (1998) (equation (8)) in Fig. 6. The failure envelopes approximated by Murff and Bransby & Randolph are both conservative with respect to the failure envelope predicted by the numerical analyses. It is noted that the failure equation presented by Bransby & Randolph was suggested for strip footings, rather than the circular footing considered here.

Horizontal-moment (HM) loading plane

A series of numerical analyses in the HM plane (with zero vertical load) was performed. The failure locus obtained from the analyses for horizontal load and moment is plotted in Fig 7. A maximum moment capacity of $M = 0{\cdot}89\ ADs_u$ is obtained, which is 11% greater than the predicted capacity of the foundation under pure moment. The maximum moment coincides with a horizontal load of $H = 0{\cdot}71\ As_u$. Application of this value of horizontal load with moment mobilizes the shear strength of more soil under the foundation during failure and therefore increases the moment capacity of the foundation. Bransby & Randolph (1998) identified two different upper-bound plasticity mechanisms for strip footings under moment and horizontal load, a scoop mechanism and a scoop–wedge mechanism. The later mechanism results in a greater ultimate moment capacity for strip footings.

A non-dimensional form of the numerically predicted failure locus and the suggestions of Murff (1994) and Bransby & Randolph (1998) are plotted in Fig. 8. It can be seen that the failure locus presented by Murff (1994) is symmetric and the maximum moment coincides with zero horizontal loading, whereas the numerical analyses show that the maximum moment is sustained with a positive horizontal load. The failure locus obtained from Murff's equation becomes non-conservative

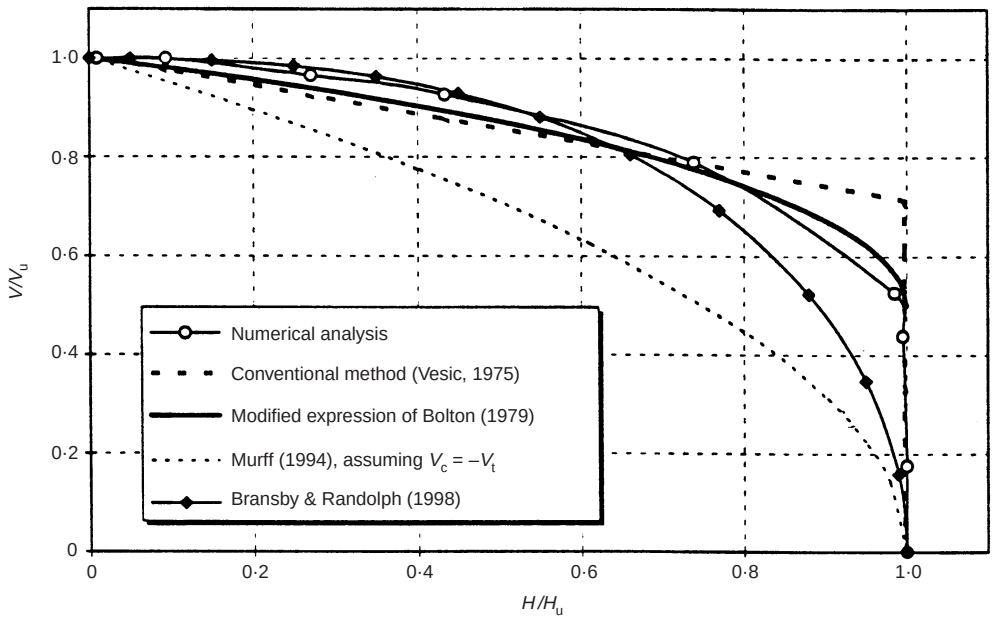

Fig. 5. Failure loci in the non-dimensional loading plane VH for foundations under inclined loading ($M = 0$)

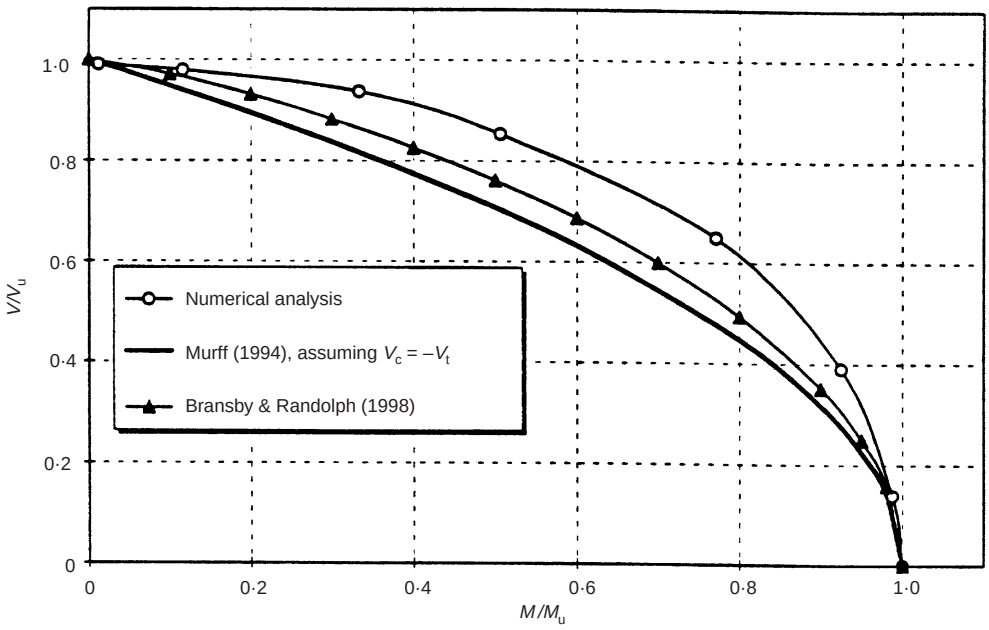

Fig. 6. Failure loci in the non-dimensional loading plane VM for foundations under eccentric loading ($H = 0$)

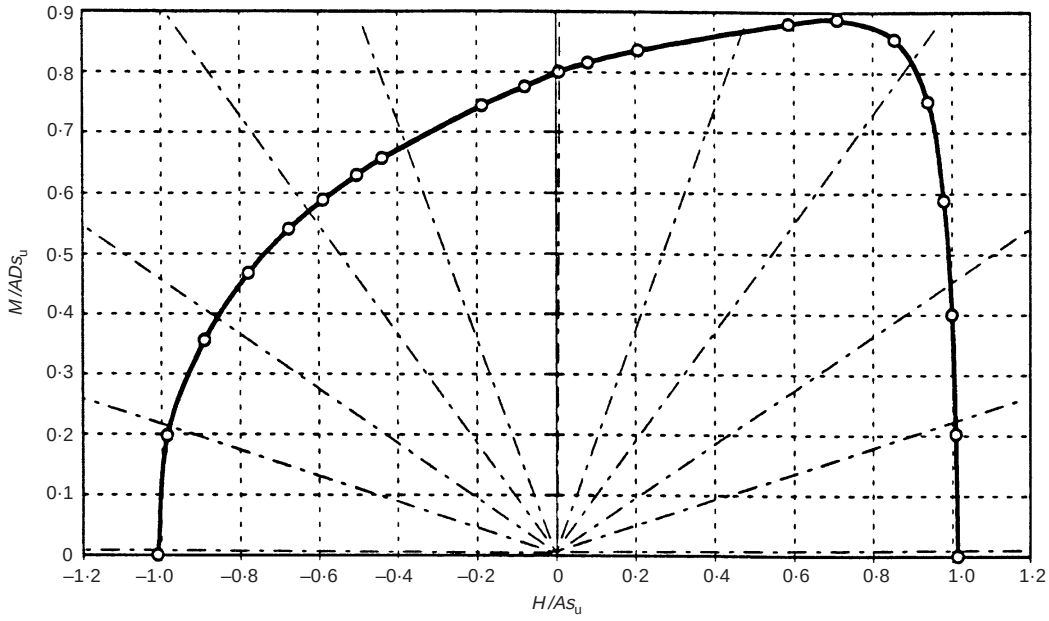

Fig. 7. Failure locus for foundations under moment and horizontal load ($V = 0$)

when $MH \leqslant 0$. The non-symmetric failure locus predicted by the current numerical technique is very similar to the failure locus obtained by Bransby & Randolph (1998) for strip footings using a finite-element analysis and upper-bound plasticity analysis.

THREE-DIMENSIONAL FAILURE ENVELOPE

Various combinations of loads and moment were used in a series of finite-element analyses to evaluate the failure envelope in VHM space. Any combination of loads with a constant ratio of horizontal load to moment H/M and varying values of vertical load V represents a line in the HM loading plane. Lines with a constant value of the ratio H/M are represented by the dashed lines in the HM plane in Fig. 7. For every selected ratio of H/M, 7–10 analyses with different values of vertical load were conducted. In each analysis, the proportional loads and moment applied to the foundation were held constant until failure.

A three-dimensional image of the failure envelope for foundations under combined compressive vertical load, horizontal load and moment is presented in Fig. 9. Representation of the failure envelope in the VMH space is shown as a contour plot in Fig. 10.

Figure 10 shows that the maximum moment is sustained when $MH > 0$. The maximum moment occurs at $H/H_u = 0{\cdot}71$ when $V = 0$. With increasing vertical load, the position of the maximum moment shifts toward the moment axis. The vertical bearing capacity of a foundation subjected to a specific horizontal load is generally larger if the moment is applied in the same direction as that of the horizontal load.

The three-dimensional representation of the failure envelope provides a convenient way to explore the safety of any specific combination of loads and moment, and the consequences of any

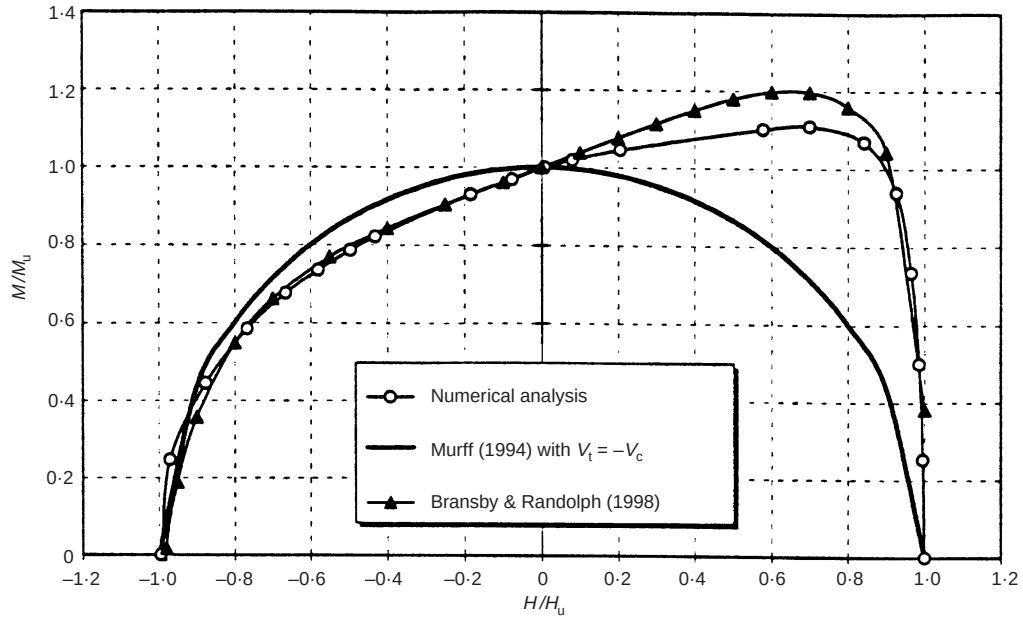

Fig. 8. Failure loci in the non-dimensional loading plane MH for foundations under moment and horizontal loading ($V = 0$)

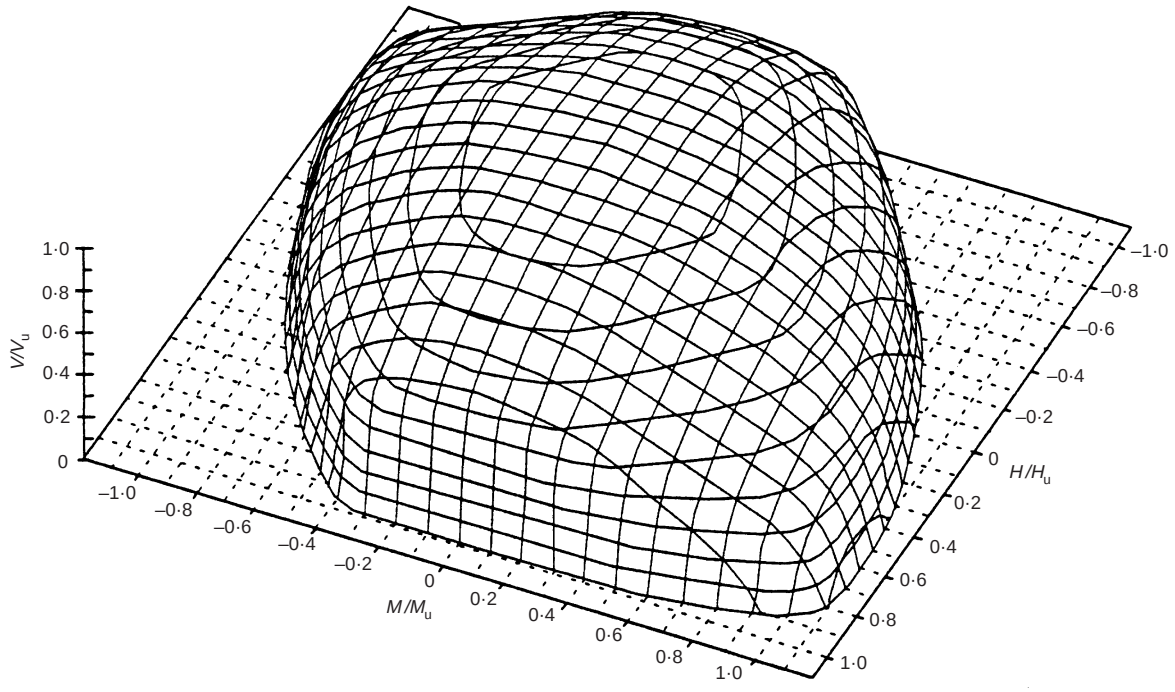

Fig. 9. Three-dimensional failure envelope in the non-dimensional space for foundations under combined loads and moment

change in the loading. Clearly the loading path has an important influence on the margin of safety. For example, consider an initial load combination of $V/V_u = H/H_u = M/M_u = 0{\cdot}4$, which is represented by point A in Fig. 10. For a foundation under maintained values of this horizontal load and moment, the maximum tolerable vertical load can be found from Fig. 10 as $V_{max}/V_u = 0{\cdot}84$. In the same way the maximum tolerable horizontal load and moment can also be found as $H_{max}/H_u = 0{\cdot}92$ and $M_{max}/M_u = 0{\cdot}95$, respectively. The minimum safety factor for the foundation under these loads is therefore 2·1 ($= 0{\cdot}84/0{\cdot}4$). If the loads and moment all increase by 25% (i.e. $V/V_u = H/H_u = M/M_u = 0{\cdot}5$) to point B in Fig. 10, the safety factor reduces to 1·5. Proportional increases of 56% to the loads and moment bring the foundation to its failure point (point C). If the initial load combination of point A is applied to the foundation and then the direction of horizontal load or moment is changed (point D), the safety factor reduces from 2·1 to 1·8.

GENERAL FAILURE EQUATION

An accurate three-dimensional equation for the failure envelope in its complete form, which accounts for the load inclination and eccentricity, is likely to be a complex algebraic expression. Some degree of simplification is essential in order to obtain a convenient form of the failure envelope. Depending on the level of the simplification, different classes of failure equations may be obtained.

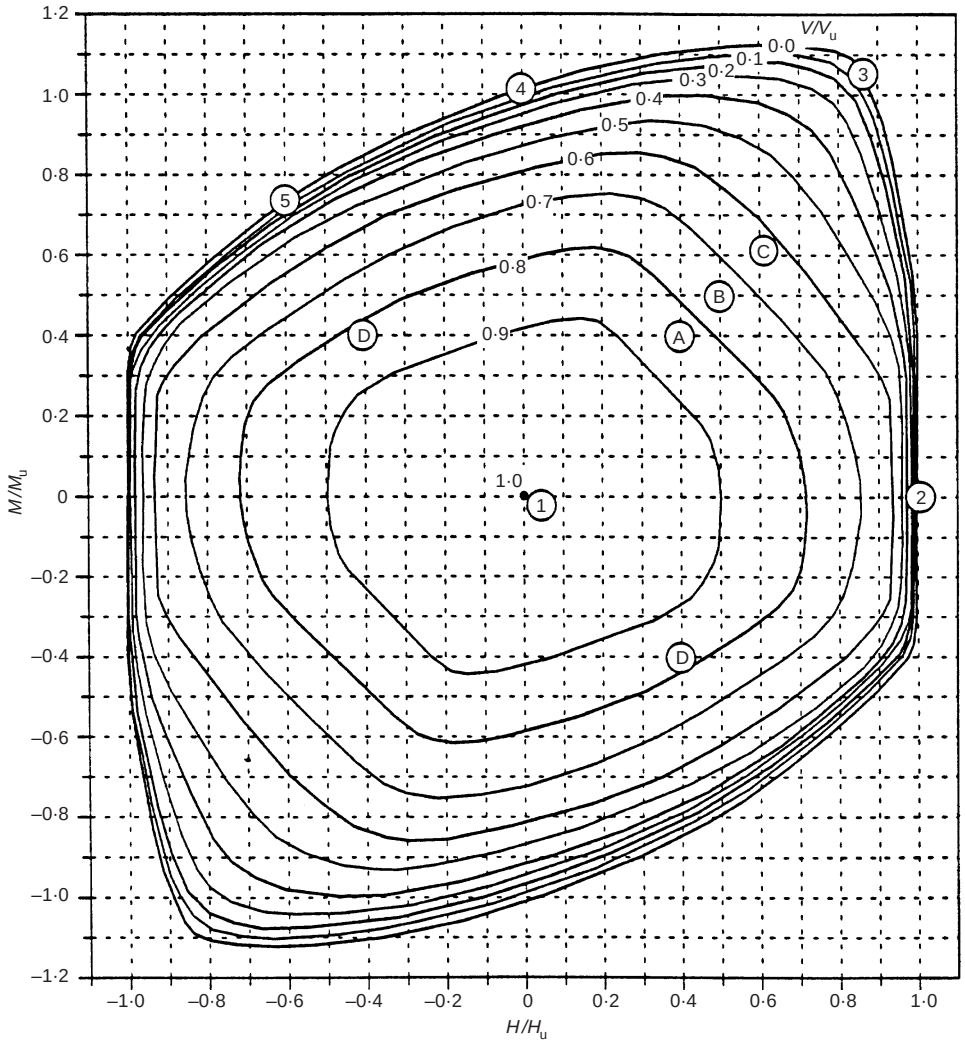

Fig. 10. Failure loci in the non-dimensional VMH space

In the previous section, the failure envelopes suggested by different sources were compared in two-dimensional loading planes. It was demonstrated that the failure equation presented by Murff (1994) has simplicity in its mathematical expression, but does not fit the failure envelopes produced by the conventional and numerical analyses. The failure equation presented by Bransby & Randolph (1998) for strip footings matches the data for circular footings in two planes, but does not give a suitable answer in three-dimensional space.

A new equation describing the failure locus in terms of all three components of the load is proposed here. In the formulation of this equation, advantage was taken of the fact that the moment capacity of the foundation is related to the horizontal load acting simultaneously on the foundation. The proposed approximate failure equation is

$$\left(\frac{V}{V_u}\right)^2+\left[\frac{M}{M_u}\left(1-\alpha_1\frac{HM}{H_u|M|}\right)\right]^2+\left|\left(\frac{H}{H_u}\right)^3\right|-1=0 \qquad (10)$$

where α_1 is a factor that depends on the soil profile. For the homogeneous soil studied here, $\alpha_1 = 0{\cdot}3$ provides a good fit to the bearing capacity predictions from the numerical analysis.

Perhaps inevitably, the three-dimensional failure locus described by equation (10) will not match the numerical data over the whole range, especially around the abrupt changes in the failure locus which occur when the horizontal load is large. However, the overall approximation to the numerical predictions is considered satisfactory, and is sufficient for many practical applications. In particular, the representation of equation (10) in the VMH space is shown as a contour plot in Fig. 11. A direct comparison of this figure with Fig. 10 shows that the proposed equation provides a very good approximation to the failure condition.

PLASTIC ZONE AND SOIL MOVEMENT

The patterns of soil movement at failure and the development of plastic zones and failure mechanisms in the soil under a footing are also of some interest. The expansion of plastic zones with increasing load and the movements of soil were studied for five cases involving different combinations of loads and moments. The various combinations of failure loads are identified in Fig. 10 as circles numbered 1–5. In all cases, the loading was applied proportionally to the foundation using an incremental load path up to the failure point.

The results of the predictions of these analyses in the plane of the applied loads are presented in Figs 12–16. The plastic zones for different ratios of the applied load to the maximum tolerable load (V/V_{max}, H/H_{max} or M/M_{max}) were obtained. The general directions of the movement of the soil particles at failure were also recorded. The patterns of movement are illustrated by curves superimposed on the cross-sections in Figs 12–16.

Plastic zones expand differently under various combinations of loads and moment. For instance, under a central vertical load the plastic zones expand to a distance of approximately $1{\cdot}0\,D$ from the centre of the footing and to a depth of $1{\cdot}5\,D$ under the foundation at failure (case 1), whereas for the foundation

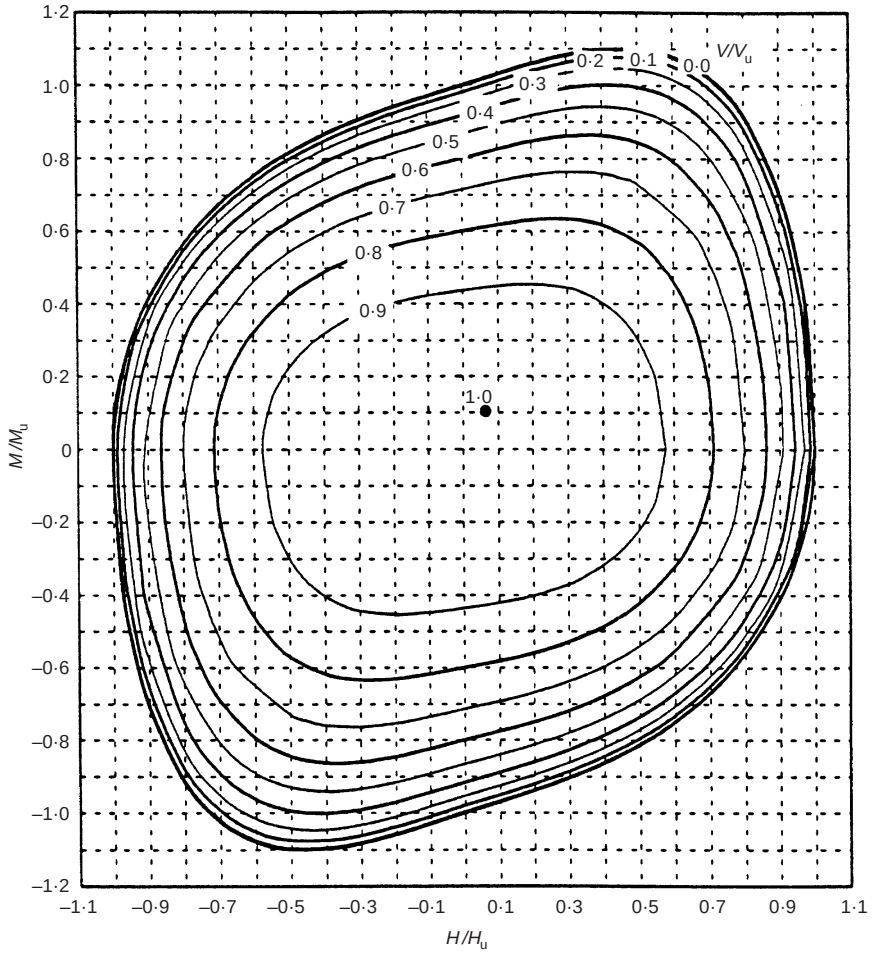

Fig. 11. Representation of the proposed failure equation in the non-dimensional VMH space

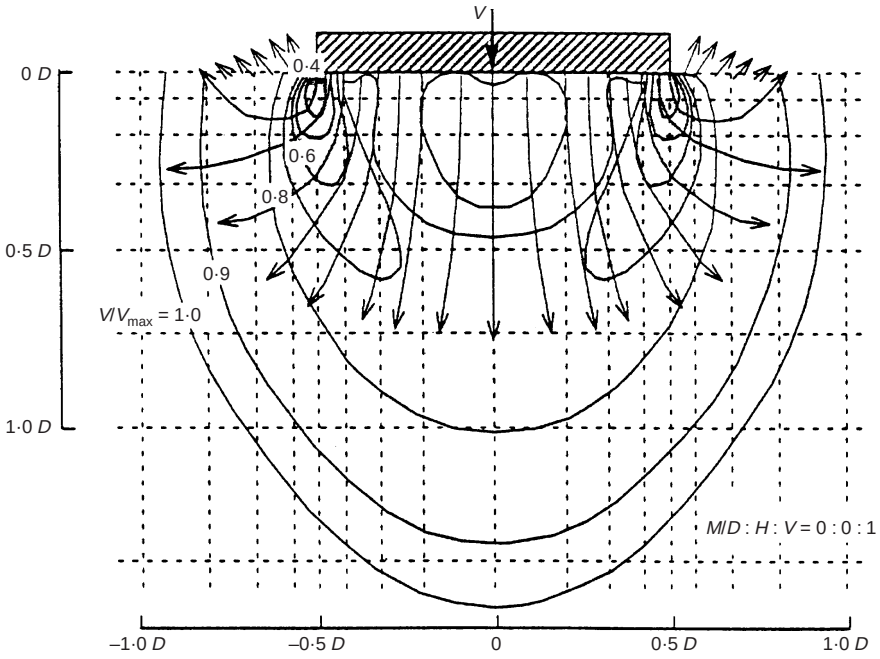

Fig. 12. Expansion of the plastic zone and direction of soil movement: case 1

under pure horizontal loading the plastic zones are concentrated under the foundation with a maximum plan size of just slightly greater than the dimension of the foundation (case 2). For a foundation subjected to moment, any increase in the horizontal load will cause the plastic zones to expand more (cases 3–5). In all cases, the soil beneath the edge of the rigid footing yields first, as might be expected. As the loads are increased, the small 'bubbles' of yielded soil beneath the edge of the footing

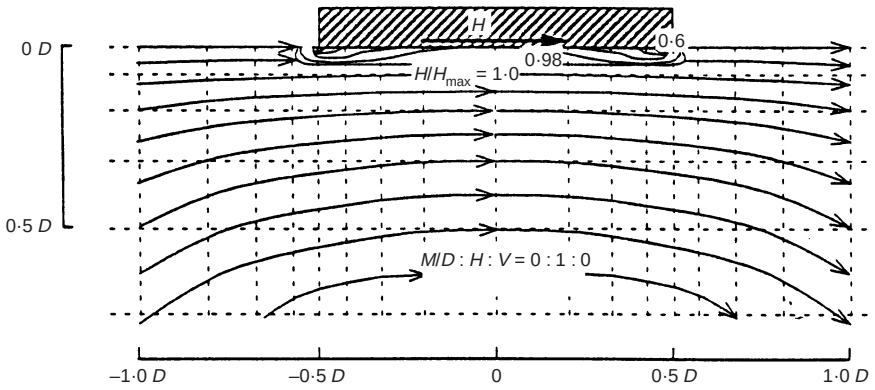

Fig. 13. Expansion of the plastic zone and direction of soil movement: case 2

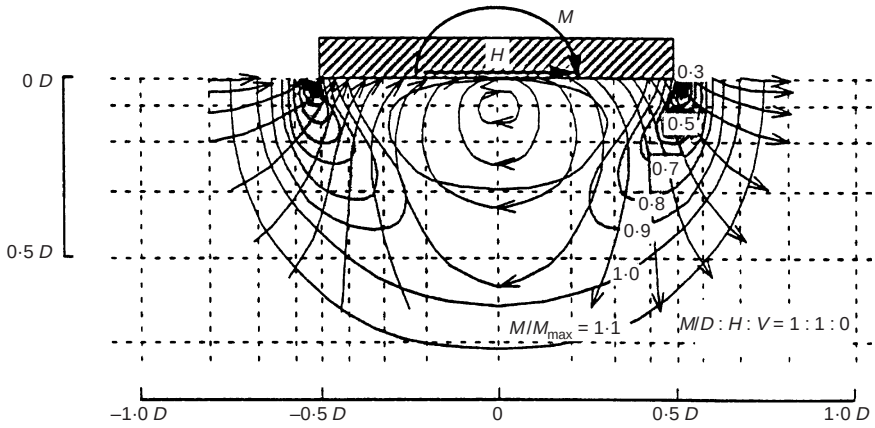

Fig. 14. Expansion of the plastic zone and direction of soil movement: case 3

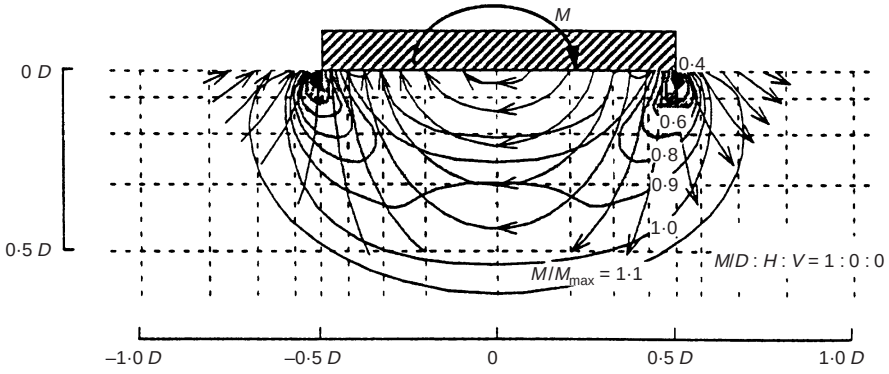

Fig. 15. Expansion of the plastic zone and direction of soil movement: case 4

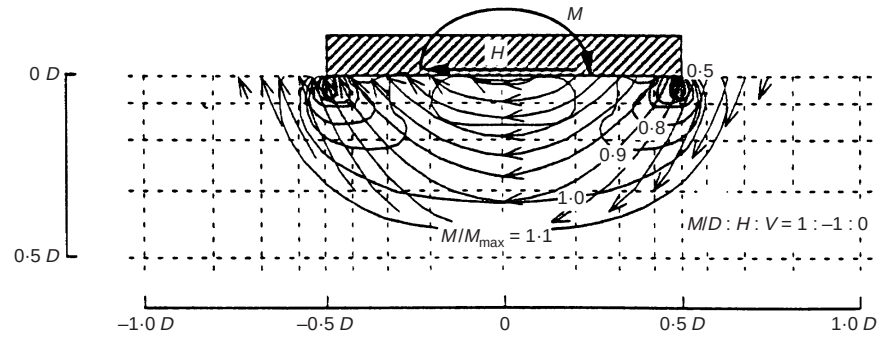

Fig. 16. Expansion of the plastic zone and direction of soil movement: case 5

expand. Eventually the plastic zone spreads over the whole area under the foundation, ultimately providing a collapse mechanism.

For foundations under moment and lateral load, there exists a point around which the foundation and soil tend to rotate. The position of this rotation point depends on the relative intensities of the applied moment and the horizontal load. Under pure horizontal load (case 2) the rotation point is in the soil far below the foundation. Application of moment brings the rotation point up, closer to the foundation (case 3). At a certain ratio of the applied moment to the horizontal load, the rotation point reaches the interface of the soil and foundation. This ratio effectively determines the extent of the plastic zone and, therefore, the maximum moment capacity for the foundation. Reducing the horizontal force and increasing the moment brings the rotation point above the foundation base. For instance, under pure moment (case 4), or when the direction of applied moment and applied horizontal force are opposite (case 5), the rotation point moves above the foundation base, the moment capacity reduces, and the plastic zone becomes smaller than the one corresponding to the maximum moment capacity.

The plastic zone and the movement of soil are not symmetrical when a combination of vertical load, horizontal load and moment is applied to the foundation.

CONCLUSIONS

Three-dimensional finite-element analyses of circular foundations on a homogeneous, purely cohesive soil were performed to investigate the shape of the undrained failure locus for the foundation. The results of the numerical analyses were compared with some of the available theoretical solutions for the undrained bearing capacity of the foundation.

Two- and three-dimensional failure loci for the foundation, deduced from the finite-element analyses, have been presented here. The failure loci provide a convenient way to investigate the undrained bearing capacity of a foundation under combined loading. Graphical displays of these loci present a clear image of the safety margin of a foundation under any specific combination of loads and moment, and the consequences of any change in the loading. It was found that the failure locus in the MH plane is non-symmetrical. The foundaton shows a higher resistance when moment and horizontal load acting on the foundation are in the same direction (i.e. both have positive or both have negative values). It was also shown that shallow foundations are most vulnerable to horizontal load and moment if the vertical load is higher than about $0{\cdot}5\ V_u$.

Another important outcome of the numerical studies is that the conventional method of calculating bearing capacity does not always give a conservative prediction. The approximate numerical results indicate that the widely accepted value of the shape factor $\zeta_s = 1{\cdot}2$, used in the conventional method may be slightly high for circular footings. The finite-element calculations indicate that a more appropriate value for the shape factor may be $\zeta_s = 1{\cdot}1$, as suggested by Meyerhof (1980). However, it is difficult to be definitive on this issue, since the technique used to determine the failure point in the numerical analyses is not completely rigorous. The conventional method also gives a non-conservative bearing capacity for foundations under large horizontal loads.

The non-dimensional failure loci predicted by the finite-element analysis are broadly similar to those obtained by Bransby & Randolph (1998) in their studies on shallow strip foundations on non-homogeneous soil. Results of experimental studies by Martin (1994) and Butterfield & Gottardi (1994) also show similar trends in behaviour for shallow foundations of different shapes on different soil profiles. This indicates that the definition of a single general bearing-capacity equation, or the failure function (e.g. equation (10)) for all types of shallow foundation may be feasible.

ACKNOWLEDGEMENTS

The research described in this paper was conducted as part of the work of the Special Research Centre for Offshore Foundation Systems, established and supported under the Australian Research Council's Research Centres Program. The support of the Centre for Geotechnical Research at the University of Sydney is also gratefully acknowledged.

REFERENCES

Bolton, M. (1979). *A guide to soil mechanics*. London: MacMillan.

Bowles, J. E. (1982). *Foundation analysis and design*, 3rd edn. New York: McGraw-Hill.

Bransby, M. F. & Randolph, M. F. (1998). Combined loading of skirted foundations. *Géotechnique* **48**, No. 5, 637–655.

Butterfield, R. & Gottardi, G. (1994). A complete three-dimensional failure envelope for shallow footing on sand. *Géotechnique* **44**, No. 1, 181–184.

Butterfield, R., Houlsby, G. T. & Gottardi, G. (1997). Standardized sign conventions and notation for generally loaded foundations. *Géotechnique* **47**, No. 5, 1051–1054.

Chen, W. F. & McCarron, W. O. (1991). *Foundation engineering handbook* (ed. H.-Y. Fang), 2nd edn, pp. 144–165. New York: Van Nostrand Reinhold.

Cox, A. D. (1961). Axially-symmetric plastic deformation in soils – II. Indentation of ponderable soils. *Int. J. Mech. Sci.* **4**, 371–380.

Cox, A. D., Eason, G. & Hopkins, H. G. (1961). Axially-symmetric plastic deformation in soils. *Proc. R. Soc. (London), Ser. A* **254**, 1.

Eason, G. & Shield, R. T (1960). The plastic indentation of a semi-infinite solid by a perfectly rough circular punch. *ZAMP* **11**, 33–43.

Lai, J. Y. & Booker, J. R. (1991). Application of discrete Fourier series to the finite element stress analysis of axi-symmetric solids. *Int. J. Numer. Methods Engng* **31**, 619–647.

Martin, C. M. (1994). *Physical and numerical modelling of offshore foundations under combined loads*. PhD thesis, University of Oxford.

Meyerhof, G. G. (1951). The ultimate bearing capacity of foundations. *Géotechnique* **2**, 301–332.

Meyerhof, G. G. (1980). Limit equilibrium plasticity in soil mechanics. *Proceedings of a symposium on application of plasticity and generalized stress–strain in geotechnical engineering*, pp. 7–24. ASCE New York.

Murff, J. D. (1994). Limit analysis of multi-footing foundation systems. *Proceedings of computer methods and advanced geomechanics, Morgantown* (eds H. J. Siriwardane & M. M. Zaman), pp. 233–244 Rotterdam.

Osborne, J. J., Trickey, J. C., Houlsby, G. T. & James, R. G. (1991). Findings from a joint industry study on foundation fixity of jackup units. *Proc 7th Offshore Technol. Conf., Houston* **3**, 517–533.

Prandtl, L. (1921). Uber die eindringungsfestigkeit plastisher baustoffe und die festigkeit von schneiden. *Z. Angew. Math. Mech*. **1**. No. 1, 15–20.

Reissner, H. (1924). Zum erddruckproblem. *Proc. 1st Int. Conf. Appl. Mech., Delft*, 295–311.

Shield, R. T. (1955). On the plastic flow of metals under conditions of axial symmetry. *Proc. R. Soc. (London), Ser. A* **233**, 267–287.

Taiebat, H. A. (1999). *Three dimensional liquefaction analysis of offshore foundations*. PhD thesis, Univeristy of Sydney.

Tani, K. & Craig, W. H. (1995). Bearing capacity of circular foundations on soft clay of strength increasing with depth. *Soils Found*. **35**. No. 4, 21–35.

Terzaghi, K. & Peck, R. B. (1948). *Soil mechanics in engineering practice*, 2nd edn. London: Wiley.

Vesic, A. S. (1973). Analysis of ultimate loads of shallow foundations. *J. Soil Mech. Found. Div., ASCE* **99**, No. SM1, 45–73

Vesic, A. S. (1975). Bearing capacity of shallow foundations. *Foundation engineering handbook* (eds Winterkorn & Fang), pp. 121–147. New York: Van Nostrand Reinhold.

Zienkiewicz, O. C. & Taylor, R. L. (1989). *The finite element method*, 4th edn. New York: McGraw-Hill.